AMERICAN ACADEMY OF OPHTHALMOLOGY®

Clinically Significant Nonperfusion Areas on Widefield OCT Angiography in Diabetic Retinopathy

Kentaro Kawai, MD, Tomoaki Murakami, MD, PhD, Yuki Mori, MD, Kenji Ishihara, MD, PhD, Yoko Dodo, MD, PhD, Noriko Terada, MD, Keiichi Nishikawa, MD, Kazuya Morino, MD, Akitaka Tsujikawa, MD, PhD

Purpose: To investigate the distribution of clinically significant nonperfusion areas (NPAs) on widefield OCT angiography (OCTA) images in patients with diabetes.

Design: Prospective, cross-sectional, observational study.

Participants: One hundred and forty-four eyes of 114 patients with diabetes.

Methods: Nominal 20 × 23 mm OCTA images were obtained using a swept-source OCTA device (Xephilio OCT-S1), followed by the creation of en face images 20-mm (1614 pixels) in diameter centering on the fovea. The nonperfusion squares (NPSs) were defined as the 10 × 10 pixel squares without retinal vessels, and the ratio of eyes with the NPSs to all eyes in each square was referred to as the NPS ratio. The areas with probabilistic differences (APD) for proliferative diabetic retinopathy (PDR) and nonproliferative diabetic retinopathy (NPDR) (APD[PDR] and APD[NPDR]) were defined as sets of squares with higher NPS ratios in eyes with PDR and NPDR, respectively. The *P* ratio (NPSs within APD[PDR] but not APD[NPDR]/all NPSs) was also calculated.

Main Outcome Measures: The probabilistic distribution of the NPSs and the association with diabetic retinopathy (DR) severity.

Results: The NPSs developed randomly in eyes with mild and moderate NPDR and were more prevalent in the extramacular areas and the temporal quadrant in eyes with severe NPDR and PDR. The APD(PDR) was distributed mainly in the extramacular areas, sparing the areas around the vascular arcades and radially peripapillary capillaries. The APD(PDR) contained retinal neovascularization more frequently than the non-APD(PDR) ($P = 0.023$). The *P* ratio was higher in eyes with PDR than in those with NPDR ($P < 0.001$). The multivariate analysis designated the *P* ratio (odds ratio, 8.293×10^7; 95% confidence interval, 6.529×10^2–1.053×10^{13}; $P = 0.002$) and the total NPSs (odds ratio, 1.002; 95% confidence interval, 1.001–1.003; $P < 0.001$) as independent risk factors of PDR. Most eyes with NPDR and 4-2-1 rule findings of DR severity had higher *P* ratios but not necessarily greater NPS numbers.

Conclusions: The APD(PDR) is uniquely distributed on widefield OCTA images, and the NPA location patterns are associated with DR severity, independent of the entire area of NPAs.

Financial Disclosure(s): Proprietary or commercial disclosure may be found after the references. *Ophthalmology Science 2023;3:100241*

Supplemental material available at www.ophthalmologyscience.org.

Diabetic retinopathy (DR) is a leading cause of visual impairment in the working age in developed countries.[1] DR is characterized by structural and functional alterations of the retinal circulation.[2] Retinal ischemia is associated with DR progression, and the concomitant expression of VEGF promotes vision-threatening DR, that is, proliferative diabetic retinopathy (PDR) and diabetic macular edema.[1,3] Therefore, automatic and objective quantification methods for nonperfusion areas (NPAs) in patients with DR may help to further identify referable disease.

Each DR case may have a unique distribution of NPAs, which can appear to develop and progress at random. Several fundus findings are associated with specific capillary nonperfusion. Cotton-wool spots correspond to focal NPAs, and most intraretinal microvascular abnormalities (IRMAs) are accompanied with NPAs in their peripheral areas.[4,5] Lamellar NPAs seem to exacerbate neurodegeneration in the inner retina and edematous changes in the middle layers.[6] Several perfusion and nonperfusion indices are associated with visual acuity (VA) and have been proposed to characterize diabetic

https://doi.org/10.1016/j.xops.2022.100241
ISSN 2666-9145/22

macular ischemia.[7] These previous publications implicate the importance of nonperfusion indices; however, the mechanisms and patterns of the distribution of NPAs during the progression of DR remains unknown.

Fluorescein angiography (FA) is the gold standard for the assessment of DR,[8] although it is an invasive and time-consuming method. The automatic detection of NPAs via FA is difficult because of background choroidal fluorescence and dye leakage from neovascularization (NV), damaged retinal vessels, and changes in signal levels in the retinal vessels over time. The clinical application of OCT angiography (OCTA), a technique that isolates the microvascular circulation in OCT image data by detecting the motion contrast of blood flow, allows for noninvasive evaluations of both the retinal and choroidal vasculature.[9,10] Because high-resolution OCTA images delineate retinal vessels selectively with less background noise, OCTA may be more feasible to detect NPAs than FA.[11] However, few studies have objectively evaluated the geometric distribution of NPAs using widefield OCTA in patients with DR.[12,13]

In this study, we investigated the distribution of clinically significant NPAs that were stochastically determined using widefield OCTA images and evaluated their associations with DR severity.

Methods

Participants

This prospective, observational, cross-sectional case series was approved by the Kyoto University Graduate School and Faculty of Medicine Ethics Committee and adhered to the tenets of the Declaration of Helsinki. Written informed consent was obtained from each participant before the study.

We enrolled patients with diabetes mellitus who were examined at the Department of Ophthalmology in Kyoto University Hospital between January 2021 and January 2022. Individuals with diabetes for whom widefield OCTA images of sufficient quality were obtained were included in the study if they provided written informed consent. The exclusion criteria were the presence of media opacities interfering with VA or image acquisition, other chorioretinal diseases, cataract surgery within 3 months, a history of vitrectomy, prior anti-VEGF treatment, and prior ocular steroid treatment; and an axial length < 22 mm or > 26 mm. Eyes with weak signal strength (< 5) or severe image artifacts on en face OCTA images were also excluded. As a result, several eyes received prior panretinal photocoagulation (PRP).

OCT Angiography

All patients underwent comprehensive ophthalmic examinations, and the best-corrected decimal VA was measured and converted into a logarithm of the minimum angle of resolution. The axial length was measured using partial coherence interferometry (IOL Master, Carl Zeiss Meditec, Inc). Ultra-widefield color fundus photographs using Optos 200Tx (Optos PLC) were obtained and graded for DR severity according to the International Clinical Disease Severity Scale for Diabetic Retinopathy.[14] Two retinal specialists (T.M. and K.K.) evaluated fundus findings and the severity grades using the photographs, and any disagreements were discussed until the specialists reached an agreement.

Two en face, swept source OCTA images centered on the upper and lower quadrants were obtained by moving the internal target upward and downward with a scanning area of nominal 20 (height) $\times$ 23 (width) mm (1614 $\times$ 1856 pixels) using a Xephilio OCT-S1 device (Canon). En face combined images of superficial and deep layers (from the internal limiting membrane to the outer plexiform layer) were generated using the default setting and, after the application of artificial intelligence–based denoising,[15] a montage image was created from 2 images using the built-in manufacturer's software (Fig 1A, B).

Assessment of the NPA Distribution and Its Relationship with Clinical Findings

The 1614-pixel (nominal 20-mm) diameter circle centered on the fovea in the images were evaluated. The images of the left eye were inverted horizontally to position the nasal subfield on the right-hand side. The 100-pixel diameter circle centered on the optic disc was excluded from the evaluation of NPAs. Vessel edges were automatically detected using the Canny Edge Detector plugin (Gaussian kernel radius = 1.5, low threshold = 2.5, and high threshold = 7.5) of ImageJ software (NIH, http://imagej.nih.gov/ij/) (Fig 1C, D),[16] after the optimization of each parameter. The image was divided into squares of 10 $\times$ 10 pixels (Fig 1E–H). The pixels of vessel edges were automatically counted in each 10 $\times$ 10 pixels square using ImageJ. The squares with no pixels of vessel edges were defined as nonperfusion squares (NPSs).

The differences in NPSs between nonproliferative diabetic retinopathy (NPDR) and PDR were investigated. For each square, the NPS ratio for each DR severity grade was defined as follows:

$$\text{NPS ratio} = \frac{\text{The number of eyes with NPSs}}{\text{The number of all eyes}}$$

The squares in which the differences in the NPS ratios between the groups were large (greater than the median) were categorized as areas with probabilistic differences (APD). The APDs between the no apparent retinopathy group and the DR group; between the no apparent retinopathy group and the NPDR group; and between the NPDR group and the PDR group were termed APD(DR), APD(NPDR), and APD(PDR), respectively. Furthermore, *clinically significant NPAs* were defined as the NPAs in APD(PDR) but not APD(NPDR).

We planned to validate the clinical relevance of the APD. The leave-one-out cross-validation method was selected to avoid overfitting. Briefly, 1 eye was first left out, and the NPS ratio of each square was calculated in the remaining eyes to determine the APD(PDR) and APD(NPDR). The NPSs in the APD(PDR) or APD(NPDR) were counted and evaluated in the left-out eye. These procedures were repeated for all eyes.

In each eye, the number of NPSs within the APD was examined. When we investigated the distribution and the extents of NPSs in each DR stage, we found several PDR cases with a smaller number of NPSs. In addition, the NPSs were distributed uniquely in eyes with PDR, compared with eyes with NPDR. This suggests that the progression to PDR or the NPA progression after NV development depends on not only the extent but also the location of NPAs. To test this hypothesis, we defined the ratios of NPSs

specific to PDR as the *P* ratio. The *P* ratio and N ratio were calculated as follows:

$$\text{P ratio} = \frac{\text{The number of NPSs in APD(PDR) but not in APD(NPDR)}}{\text{The total number of NPSs}}$$

$$\text{N ratio} = \frac{\text{The number of NPSs in APD(NPDR) but not in APD(PDR)}}{\text{The total number of NPSs}}$$

The location of the NV was determined in 3-dimensional OCTA images, as described previously.[17] Neovascularization within 1 disc-radius value from the disc was defined as neovascularization of the disc (NVD). Other NV was defined as retinal neovascularization (NVE).

Statistical Analyses

All values were expressed as median and interquartile range (IQR). Statistical significance was set at $P < 0.05$. The agreement of qualitative parameters was assessed using the κ coefficient. Mann−Whitney *U* tests and Kruskal-Wallis test with Bonferroni correction were performed to compare continuous variables. Fisher exact test or chi-square test was used to compare categorical variables. Spearman's correlation coefficient was used to analyze the association between the 2 continuous variables.

Multivariable logistic regression analysis (independent variables = number of NPSs in whole areas and *P* ratio; dependent variable = PDR) was conducted to determine the risk factors discriminating eyes with PDR from those with NPDR. The NPSs were analyzed using the R software (version 3.6.1; R Foundation for Statistical Computing), and all statistical analyses, except for hierarchical clustering, were performed using the EZR software. Hierarchical agglomerative clustering was conducted using SPSS (version 24; IBM).

Results

The Unique Distribution of NPAs in Severe NPDR and PDR

We acquired OCTA images of 178 eyes from 139 participants with diabetes. After excluding 34 eyes because of weak signal strength or severe image artifacts, we investigated 144 eyes from 114 participants in the study (Table 1). The agreement of qualitative findings and DR grades are shown in Table S1 (available at www.ophthalmologyscience.org). The percentages of NPSs in each eye were 0.45% (IQR, 0.31−0.77) in 27 eyes with no apparent retinopathy, 0.92% (IQR, 0.48−1.58) in 15 eyes with mild NPDR, 1.00% (IQR, 0.52−1.89) in 40 eyes with moderate NPDR, 1.90% (IQR, 1.16−3.32) in 18 eyes with severe NPDR, and 5.42% (IQR, 2.55−10.12) in 44 eyes with PDR. The percentages in the extramacular sectors (nominal, 10−20 mm) were higher in eyes with severe NPDR and PDR (Fig S1, available at www.ophthalmologyscience.org).

We evaluated the perfusion status in each square of 10 × 10 pixels, and the NPS ratios were shown on pseudocolored rate map images in each DR severity grade (Fig 2). The NPSs developed at random locations in eyes with mild and moderate NPDR (Fig 2), whereas the ratios increased particularly in the extramacular areas and the temporal quadrant in eyes with severe NPDR and PDR (Fig S1). The maps of the differences in the NPS ratios between individual DR severity grades confirmed the high frequency of NPAs in these areas in the later stages (Fig S2, available at www.ophthalmologyscience.org). Pseudocolored rate map images demonstrated that 17 PDR eyes with NVD had high NPS ratios in the nasal subfield of the extramacular areas, compared with 27 PDR eyes without NVD (Fig S3, available at www.ophthalmologyscience.org).

Stochastic Determination of Clinically Significant NPAs

Fig 3A−C shows the differences in the NPS ratios for each square between no apparent retinopathy and DR, between no apparent retinopathy and NPDR, and between NPDR and PDR. The APDs in eyes with DR, NPDR, and PDR were defined after thresholding (Fig 3D-F and Fig S4, available at www.ophthalmologyscience.org). The APD(PDR) was absent around the vascular arcades, around the radial peripapillary capillaries (RPC), and in the macula except for the temporal quadrant, whereas the APD(NPDR) was randomly present throughout the retina.

The retinas were divided into the following 4 categories: (1) both APD(PDR) and APD(NPDR), (2) APD(PDR) but not APD(NPDR), (3) APD(NPDR) but not APD(PDR), and (4) neither APD(PDR) nor APD(NPDR) (Fig 3G and Figs S5 and S6, available at www.ophthalmologyscience.org).To consider the likelihood of PDR, we investigated the association of PDR with the *P* ratios or N ratios (Fig 4). Interestingly, the *P* ratios ranged from 0.08 to 0.30 in eyes with NPDR, whereas most eyes with PDR had higher ratios ($P < 0.001$; Fig 4A, Fig S7, available at www.ophthalmologyscience.org). The number of NPSs in the entire areas ranged from 129 to 6555 in eyes with PDR, although most eyes with NPDR had < 1200 NPSs ($P < 0.001$; Fig 4A). There was a significant association between the *P* ratio and the total number of NPSs ($\rho = 0.539$, $P < 0.001$). The *P* ratio (odds ratio, 8.293×10^7; 95% confidence interval, 6.529×10^2−1.053×10^{13}; $P = 0.002$) and the total number of NPSs (odds ratio, 1.002;

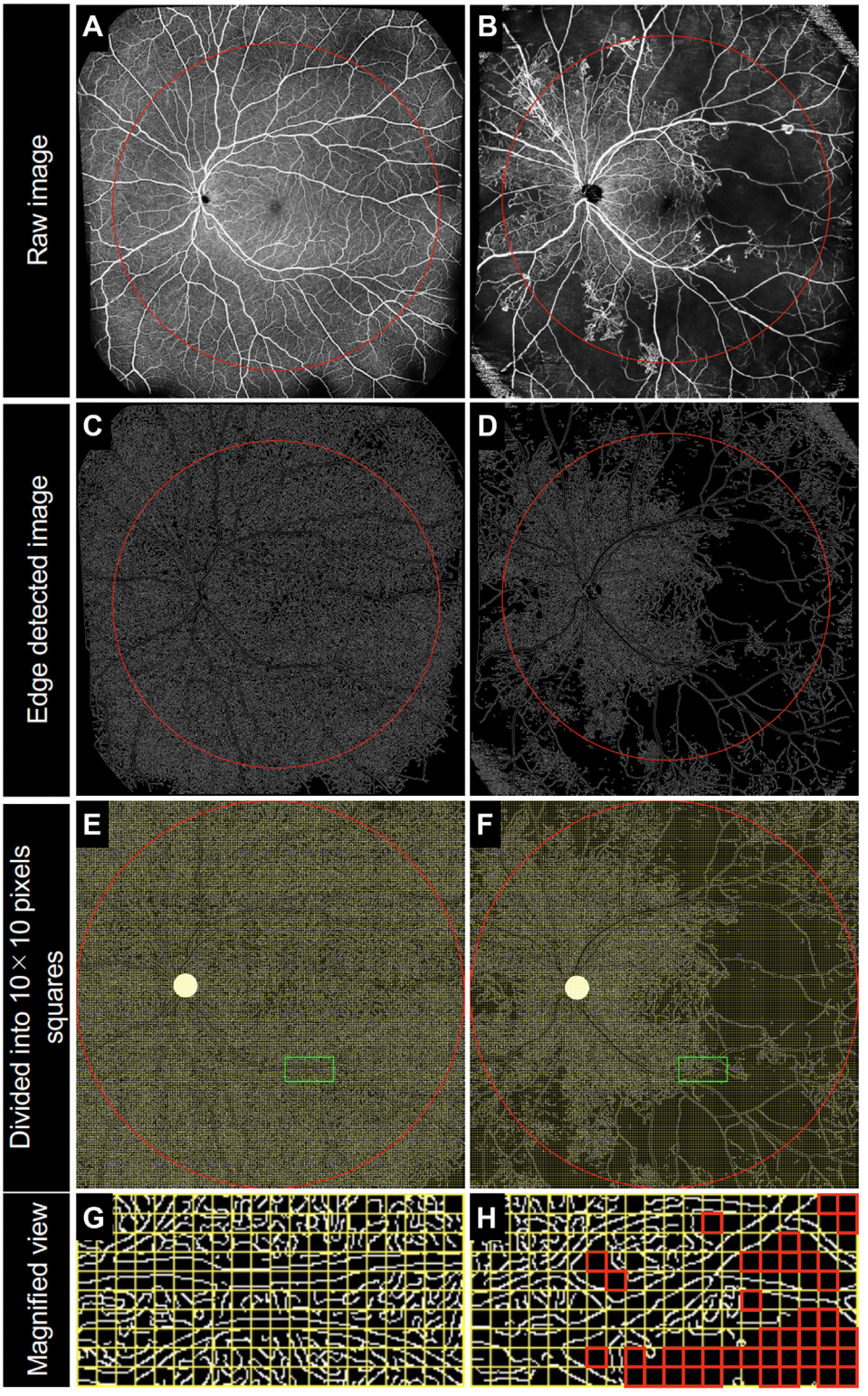

Figure 1. Semiautomatic assessment of nonperfusion areas on OCT angiography in 2 representative diabetic eyes. The left eye of a 32-year-old patient with no apparent retinopathy (**A, C, E, G**), and the left eye of a 48-year-old patient with proliferative diabetic retinopathy (**B, D, F, H**). **A, B**, The montage image of 2 en face OCT angiography images. **C, D**, The binary image using the edge detection function of the ImageJ software plugin. **E, F**, The binary image is divided into squares of 10 × 10 pixels. Magnified images of the green rectangles in panels **E** and **F** are shown in panels **G** and **H**, respectively.

Table 1. Participant Characteristics

	All Participants	No Apparent Retinopathy	NPDR	PDR
Eyes/patients	144/114	27/18	73/61	44/35
Age (y)	66 (56–73)	66 (56–74)	68 (58–73)	62 (51–68)
Sex (male/female)	79/35	9/9	42/19	28/7
Hemoglobin A1c (%)	7.2 (6.6–8.5)	8.0 (6.6–8.7)	7.1 (6.8–8.5)	7.1 (6.3–8.2)
Duration of diabetes (y)	17 (10–22)	14 (8–20)	18 (12–22)	17 (7–22)
Systemic hypertension (present/absent)	76/38	12/6	42/19	22/13
Dyslipidemia (present/absent)	62/52	14/4	28/33	20/15
Cardiovascular disease (present/absent)	13/101	2/16	6/55	5/30
Renal disease (present/absent)	38/76	7/11	21/40	10/25
Prior myocardial infarction (present/absent)	5/109	0/18	4/57	1/34
Prior stroke (present/absent)	8/106	0/18	6/55	2/33
logMAR VA	0.000 (− 0.079 to 0.046)	− 0.079 (− 0.176 to 0.023)	− 0.079 (− 0.079 to 0.000)	0.000 (0.000–0.097)
Phakia/pseudophakia	96/48	19/8	47/26	30/14
International DR severity grade (eyes/patients)				
Mild NPDR	15/13	–	15/13	–
Moderate NPDR	40/33	–	40/33	–
Severe NPDR	18/15	–	18/15	–
PDR	44/35	–	–	44/35
More than 20 intraretinal hemorrhages in each of 4 quadrants (eyes)	10	–	6	4
Definite venous beading in ≥ 2 quadrants (eyes)	19	–	6	13
Prominent intraretinal microvascular abnormalities in ≥ 1 quadrants (eyes)	43	–	13	30
Retinal neovascularization (eyes)	42	–	0	42
Neovascularization of the disc (eyes)	17	–	0	17
Prior PRP (eyes)	45	–	7	38

Data are shown as numbers or median (interquartile range).
DR = diabetic retinopathy; logMAR = logarithm of the minimum angle of resolution; NPDR = nonproliferative diabetic retinopathy; PDR = proliferative diabetic retinopathy; PRP = panretinal photocoagulation; VA = visual acuity.

95% confidence interval, 1.001−1.003; $P < 0.001$) were found to be independent risk factors of PDR.

Hierarchical clustering divided the eyes with NPDR into 2 major groups: a high-*P*-ratio group of 45 eyes and a low-*P*-ratio group of 28 eyes (Fig 5A). The *P* ratios in eyes with PDR were similar to those of eyes with NPDR of a high-*P*-ratio group. The high-*P*-ratio group had poorer logarithm of the minimum angle of resolution ($P = 0.039$), more pseudophakia ($P = 0.014$), more severe DR ($P = 0.004$), and more NPSs ($P = 0.008$) than the low-*P*-ratio group (Table 2).

Relationship between Clinically Significant NPAs and DR Severity

We evaluated the association between clinically significant NPAs and the international DR severity grades. Retinal neovascularization were delineated in the outer areas of the nasal quadrant, though they were also observed within the posterior pole in the superotemporal and inferotemporal quadrants (Fig 6). The APD(PDR) contained NVEs more frequently than the non-APD(PDR) (89 [62.2%] vs 54 [37.8%]; $P = 0.023$) (Fig 6A, B). Most eyes with 4-2-1 rule findings had higher P ratios, although the number of NPSs did not necessarily increase in these eyes (Fig 5C-E, Table 2, and Fig S8, available at www.ophthalmologyscience.org).

Discussion

In this study, we investigated the distribution of NPAs stochastically and demonstrated that the NPAs developed at random in eyes with mild and moderate NPDR, whereas

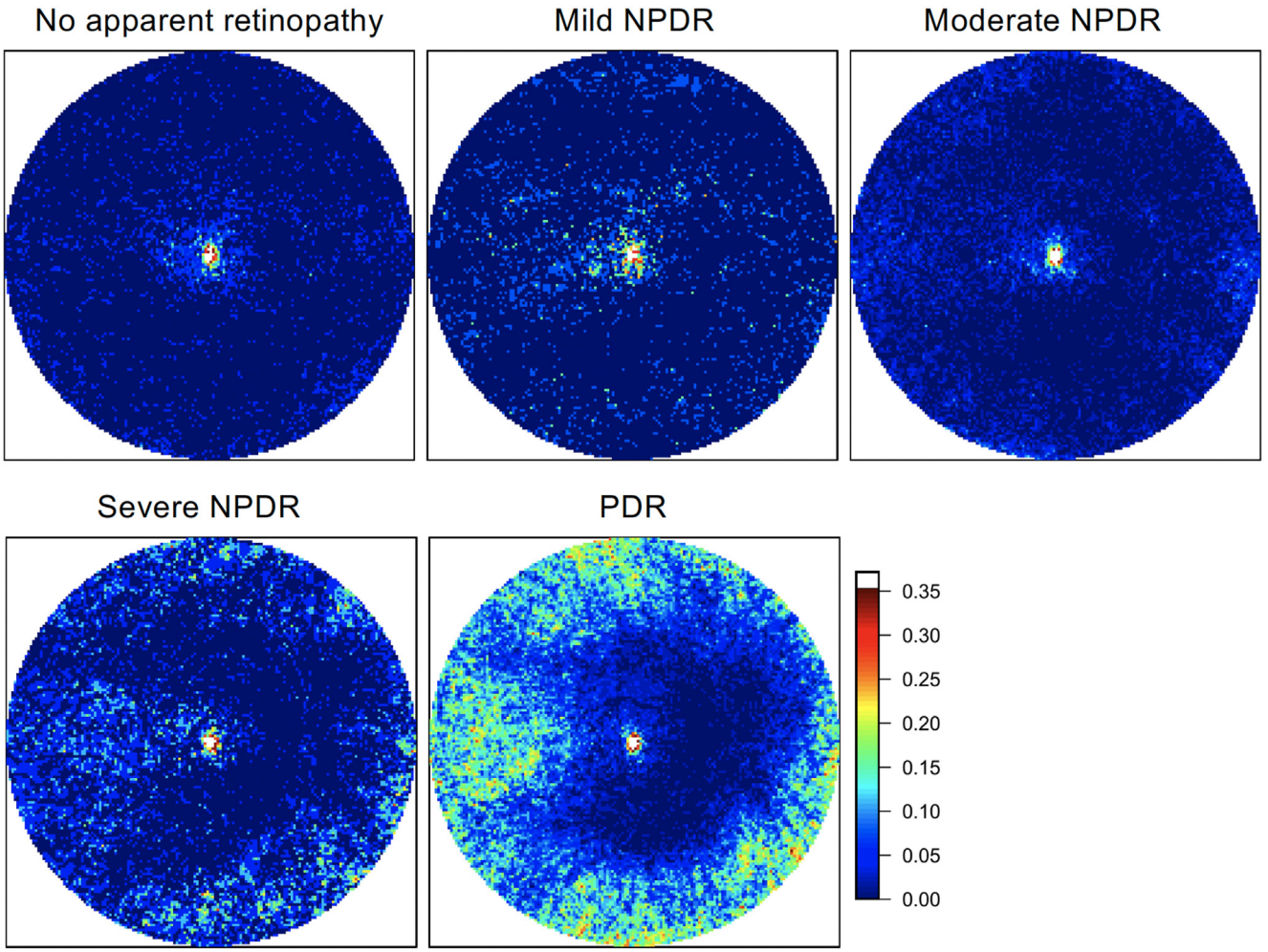

Figure 2. Ratios of the nonperfusion squares in each square based on diabetic retinopathy severity. The nonperfusion square ratios in each square in eyes with each diabetic retinopathy (DR) severity grade in pseudocolored maps. The nasal quadrant is on the right-hand side. NPDR = nonproliferative diabetic retinopathy; PDR = proliferative diabetic retinopathy.

the NPAs were distributed mainly in the extramacular areas and the temporal subfield in eyes with severe NPDR and PDR. Interestingly, the APD(PDR) were not present around the vascular arcade or RPCs and contained 62.2% of NVEs. A higher *P* ratio is a risk of PDR, independent of the NPA areas. Additionally, eyes with severe NPDR also had higher P ratios. These data might designate the NPAs in APD(PDR) but not APD(NPDR) as *clinically significant NPAs* for the progression of DR.

Previous studies that have subjectively analyzed and manually defined the NPAs using ultra-widefield FA found that the ischemic index is correlated with DR severity.[18–20] However, OCTA images with higher signal/noise ratios provide an advantage for the automatic detection of NPAs. The clinical relevance of widefield OCTA images for the discrimination of PDR and NPDR has been reported in some studies, though how widefield imaging delineates the pathogenesis of the NPAs and concomitant NV development remain unclear.[13,21] In this study, the objective and semiautomatic determination of areas and the distribution of NPAs allowed us to propose the APD and quantify the clinically significant NPAs. This image processing method can be used to determine the risks of PDR and to predict PDR development in a clinical setting. Piccolino et al[22] proposed 3 patterns of NPA distribution in eyes with PDR and reported the association between early NVE and the midperipheral capillary nonperfusion, which was observed in > 80% eyes. It may be consistent with the distribution of APD(PDR) to some extent. The objective and quantitative analyses in the current study demonstrated more precise distribution and the probability of NPAs in eyes with PDR, compared with those in eyes with NPDR.

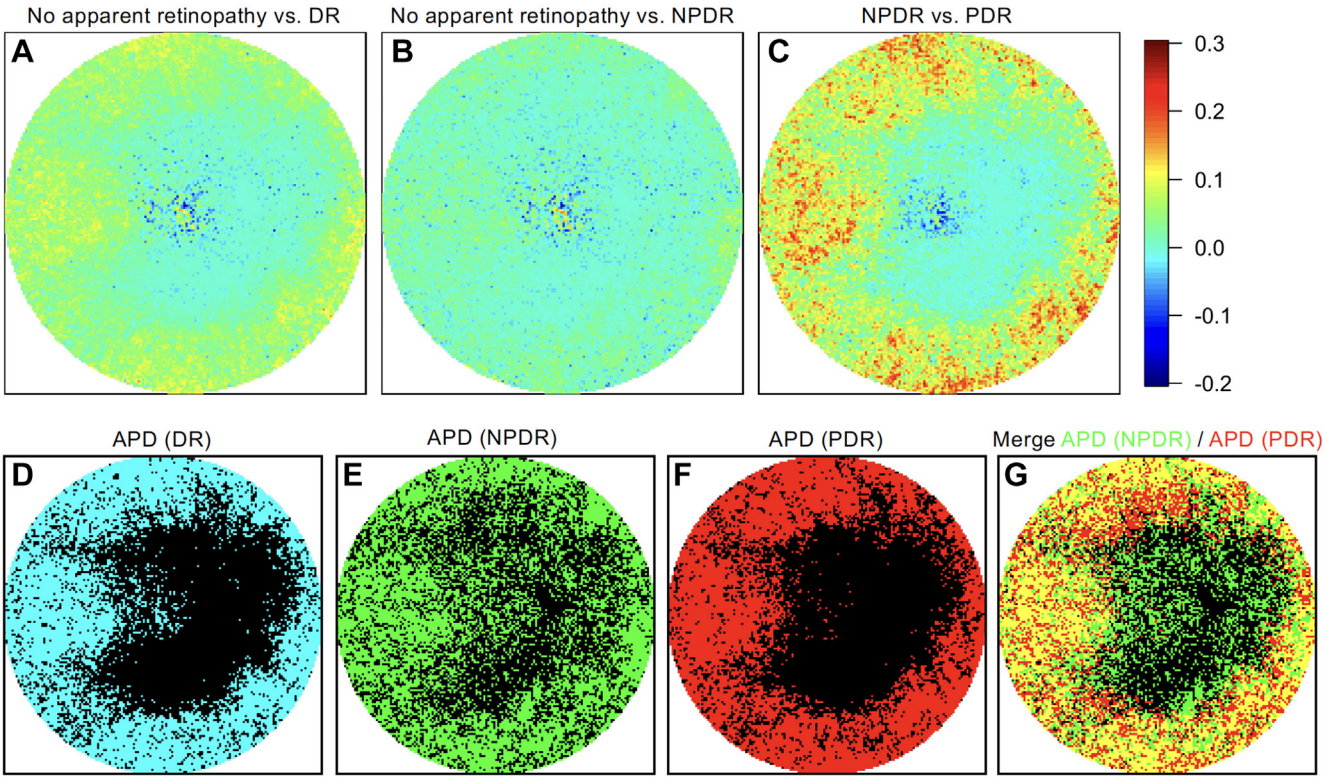

Figure 3. Probabilistic definition of clinically significant nonperfusion areas in diabetic retinopathy (DR). **A, B, C**, The differences in the ratios of nonperfusion squares (NPSs) in each square between eyes with no apparent retinopathy and those with DR (**A**), between eyes with no apparent retinopathy and those with nonproliferative diabetic retinopathy (NPDR) (**B**), and between eyes with NPDR and those with proliferative diabetic retinopathy (PDR) (**C**). The values are obtained by subtracting the NPS ratios of a milder group from those of a more severe group. **D, E, F**, After thresholding with the median, the areas with probabilistic differences (APDs) in panels **A**, **B**, and **C** were defined as the APD(DR), APD(NPDR), and APD(PDR), respectively. **G**, The merged image of APD(NPDR) and APD(PDR) shows unique distributions of APDs between the groups. The nasal quadrant is shown on the right-hand side.

It remains to be investigated in the future how the number and distribution of NPSs change after treatment with PRP or anti-VEGF injection.

Despite the clinical significance of the uniquely distributed APD(PDR), what factors determine the locations of NPAs in eyes with PDR remains unclear. The stochastic distribution of the NPSs was different between eyes with venous beading and those with IRMAs, suggesting multiple pathways to NVE development. In the posterior pole, vessels in the temporal quadrants were accompanied by fewer RPCs and had a lower perfusion pressure than those in other quadrants.[23] This may explain the imbalance of the NPAs between the nasal and temporal subfields.[24] The macula showed a lower frequency of NPAs than the extramacular area. In the macula, where the retina is thicker and has few arterioles with a large diameter, deep capillaries bridge under the arterioles and may function as collateral vessels.[25] On the other hand, in the extramacular area, large arterioles residing in both the superficial and deep layers could be the perfusion boundaries.[26] This may explain the difference in the frequency of NPAs between the macula and extramacular area. The NPA analysis of each layer would provide more detailed data, although the current widefield OCTA device does not have the sufficient accuracy in autosegmentation, especially in the periphery, and en face images of each layer with good quality were not available. Future research using improved image acquisition and processing is desired. IRMAs can serve as shunt vessels.[27] Retinal neovascularization was more frequently observed within the APD(PDR) in the current study; the severity of ischemia in the posterior pole and midperiphery reportedly correlates with NVEs.[28] Whether peripheral NPA causes these vascular lesions or the lesions cause peripheral NPA by stealing blood vessels requires further investigation.

The *P* ratio was used in this study to investigate the clinical significance of NPAs, and we observed that it was significant in the APD(PDR) but not in the APD(NPDR).

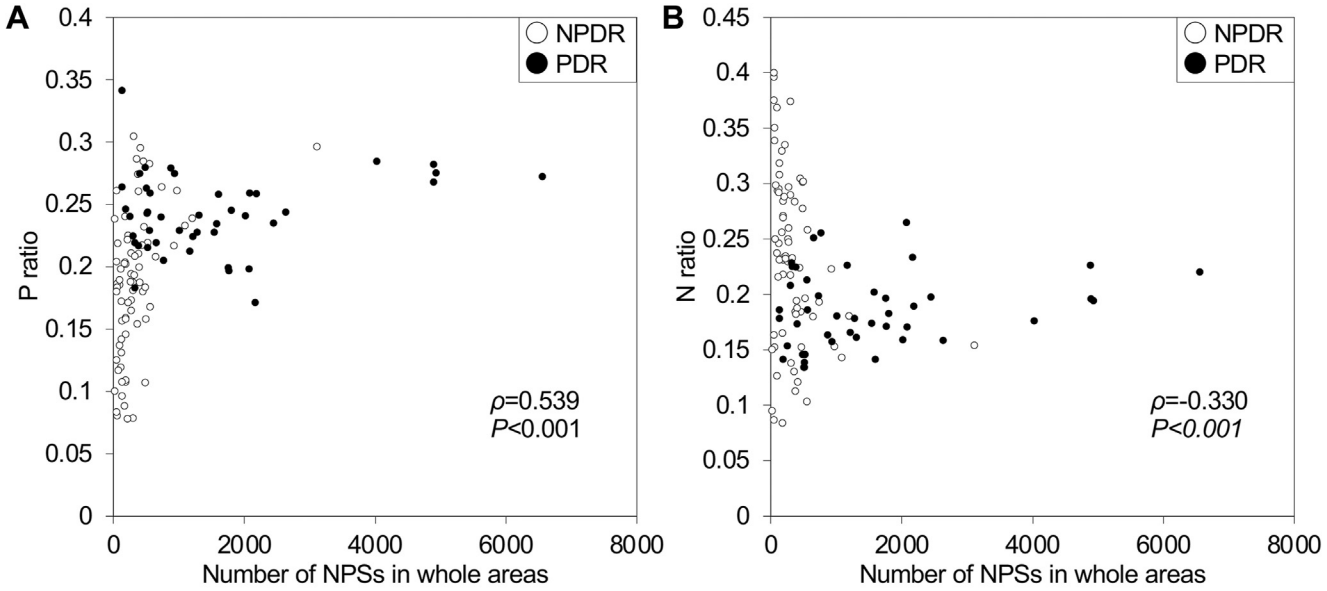

Figure 4. Relationship between number of nonperfusion squares (NPSs) and clinically significant nonperfusion areas. A scatter plot of the number of NPSs and the *P* ratios (**A**) and N ratios (**B**). Eyes with proliferative diabetic retinopathy (PDR) have higher *P* ratios and lower N ratios, although the number of NPSs is not necessarily high in eyes with PDR. NPDR = nonproliferative diabetic retinopathy.

$$\text{P ratio} = \frac{\text{The number of NPSs in APD(PDR) but not in APD(NPDR)}}{\text{The total number of NPSs}}$$

$$\text{N ratio} = \frac{\text{The number of NPSs in APD(NPDR) but not in APD(PDR)}}{\text{The total number of NPSs}}$$

The parenchyma and vasculature do not have a uniform structure throughout the retina.[26,29] Some eyes with PDR had small NPA and a higher *P* ratio, suggesting that the NPA in the APD(PDR) but not in APD(NPDR) contribute to the development of nearby NVEs. Retinal neovascularization develop mainly in the extramacular areas, and their development is dependent on several factors, such as the adherent vitreous cortex, local VEGF expression, and loss of retinal ganglion cells, which exert antiangiogenic effects.[30,31] We therefore speculate that clinically significant NPAs and the total areas of NPAs throughout the retina should be carefully evaluated during screening for PDR. Neovascularization of the disc is generally a marker of advanced PDR. In this study, PDR eyes with NVD had higher NPS ratios in the nasal subfield, whereas the NPS ratios were higher in the temporal subfield in PDR eyes without NVD. This suggests that the extramacular NPAs in the nasal side contribute to the development of NVD. Future longitudinal studies with a large number of participants should confirm the association between NVD and the locations of NPAs.

A method for identifying NPDR eyes with a high risk of progressing to PDR would be of great clinical significance. Cluster analysis revealed that NPDR eyes with higher *P* ratios were often accompanied by multiple retinal hemorrhages, venous beading, or IRMAs, which predict PDR development in the international DR severity grades. This suggests that the *P* ratios also have clinical relevance in eyes with NPDR. However, several NPDR eyes with higher *P* ratios did not have these fundus findings. Future longitudinal studies should elucidate whether higher *P* ratios are a novel predictor of progression to PDR. Eyes of the high-*P*-ratio group had pseudophakia more frequently. In this study, high *P* ratio was associated with DR severity and greater NPAs, which suggests that higher levels of VEGF expression and concomitant vascular hyperpermeability may promote cataract progression, resulting in frequent cataract surgery. Alternatively, the common regulators, for example, biochemical pathways stimulated by hyperglycemia, might contribute to cataract progression and NPA development in the APD(PDR). Intraocular inflammation after cataract surgery might promote the NPA progression there. Further studies with a larger number of patients are warranted.

This study had several limitations. First, all patients were Asians from a single center, with relatively few eyes with mild NPDR and severe NPDR, which may result in

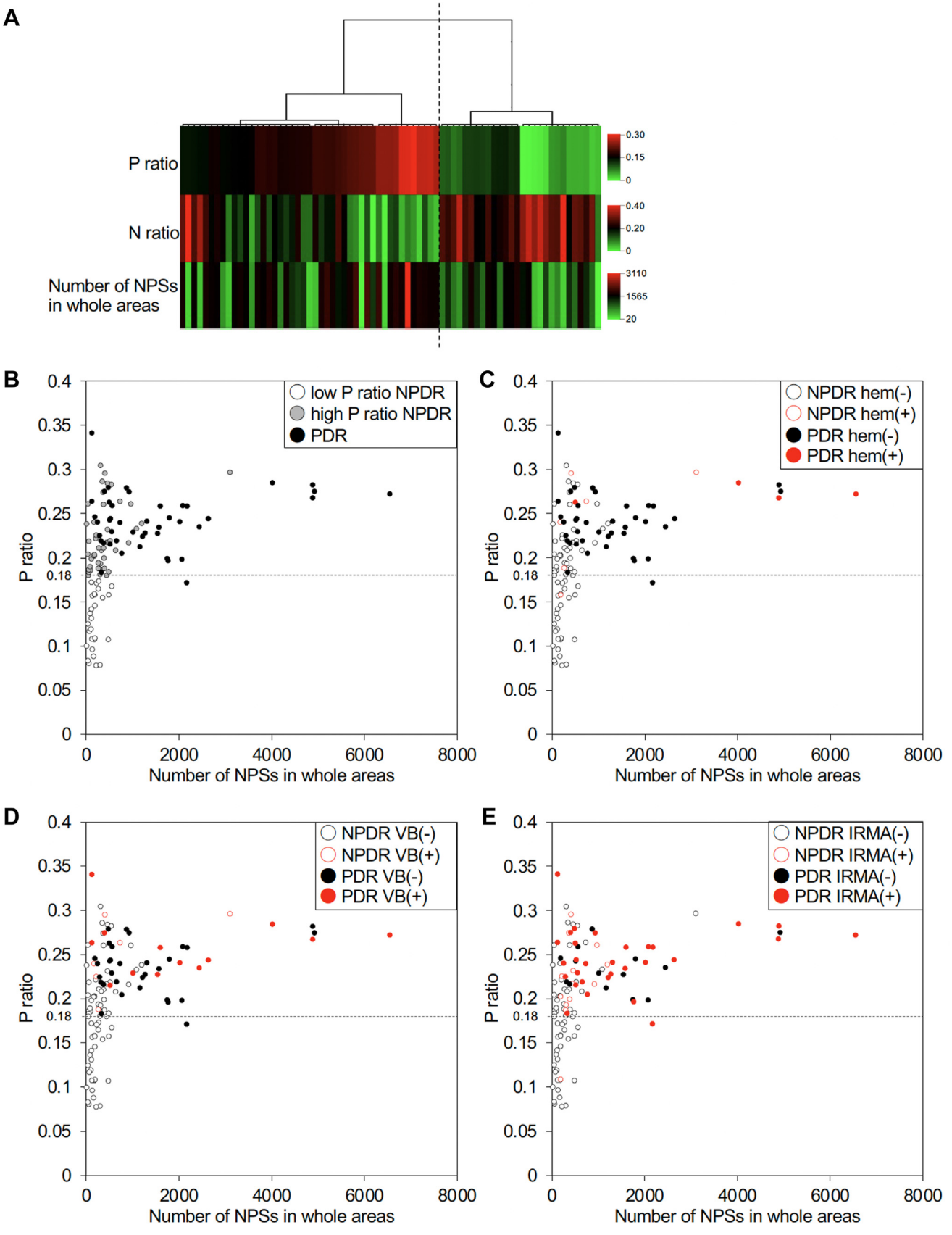
A
P ratio
N ratio
Number of NPSs in whole areas
0.30
0.15
0
0.40
0.20
0
3110
1565
20
B
low P ratio NPDR
high P ratio NPDR
PDR
P ratio
Number of NPSs in whole areas
C
NPDR hem(-)
NPDR hem(+)
PDR hem(-)
PDR hem(+)
P ratio
Number of NPSs in whole areas
D
NPDR VB(-)
NPDR VB(+)
PDR VB(-)
PDR VB(+)
P ratio
Number of NPSs in whole areas
E
NPDR IRMA(-)
NPDR IRMA(+)
PDR IRMA(-)
PDR IRMA(+)
P ratio
Number of NPSs in whole areas

Table 2. Comparisons of Each Parameter between Low and High *P* Ratio Groups in Eyes with Nonproliferative Diabetic Retinopathy

	Low-*P*-ratio group (n = 28)	High-*P*-ratio group (n = 45)	*P*
Age (y)	67 (60–73)	68 (58–76)	0.443
Sex (male/female)	21/7	30/15	0.601
Hemoglobin A1c (%)	7.1 (6.7–8.0)	7.3 (6.8–8.6)	0.305
Duration of diabetes (y)	19 (13–23)	18 (12–22)	0.579
Systemic hypertension (present/absent)	22/6	15/30	< 0.001
Dyslipidemia (present/absent)	14/14	16/29	0.235
Cardiovascular disease (present/absent)	3/25	3/42	0.669
Renal disease (present/absent)	9/19	13/32	0.798
Prior myocardial infarction (present/absent)	3/25	2/43	0.365
Prior stroke (present/absent)	3/25	6/39	1.000
logMAR VA	− 0.079 (− 0.103 to 0.059)	0.000 (− 0.079 to 0.046)	0.039
Phakia/pseudophakia	23/5	24/21	0.014
International DR severity grade (eyes)			0.004
Mild NPDR	10	5	
Moderate NPDR	16	24	
Severe NPDR	2	16	
More than 20 intraretinal hemorrhages in each of 4 quadrants (present/absent)	1/27	5/40	0.396
Definite venous beading in ≥ 2 quadrants (present/absent)	0/28	6/39	0.076
Prominent intraretinal microvascular abnormalities in ≥ 1 quadrants (present/absent)	1/27	12/33	0.012
NPSs number of NPAs in whole areas	178 (117–239)	316 (179–461)	0.008

Data are shown as numbers or median (interquartile range).
DR = diabetic retinopathy; logMAR = logarithm of the minimum angle of resolution; NPA = nonperfusion area; NPDR = nonproliferative diabetic retinopathy; NPS = nonperfusion square; PDR = proliferative diabetic retinopathy; VA = visual acuity.

selection bias. A few parameters have been shown to be associated with the retinal vascular metrics. In particular, we did not find an association of the number of NPSs with age and axial length (data not shown), although we did not completely exclude the effects of these confounders in the statistical analyses. Because patients with prior PRP were not excluded, the natural course of DR was not necessarily analyzed. Although no reperfusion of vessels or capillary network was detected in the short to medium term after PRP,[32] PRP has been reported to cause retinal oxygenation,[33] intraocular VEGF reduction,[34] and vasoconstriction,[35] which may affect NPA distribution. Second, the widefield OCTA images do not completely correspond to the anatomic images of retinal vasculature after artificial intelligence–based denoise processing.[5,15] Distortions from the spherical surface to the plane could not be corrected; therefore, the approximate values were analyzed. In addition, the length of one pixel on the retina was not strictly consistent among different eyes, and the areas of a 10 × 10 pixel square were varied after the correction for the axial length according to the Littman-Bennett formula (14 817 ± 1213 μm^2).[36,37] Further, refraction, including astigmatism, should also be taken into account. Third, the areas of NPA might have been

Figure 5. Two major patterns of location of nonperfusion areas in eyes with nonproliferative diabetic retinopathy (NPDR). **A**, A dendrogram of hierarchical clustering by *P* ratios in eyes with NPDR is shown. Unsupervised clustering divides 73 eyes with NPDR into 2 major groups: a high-*P*-ratio group (n = 45 eyes) and a low-*P*-ratio group (n = 28 eyes). The threshold of the *P* ratios is 0.18. **B**, The *P* ratios in eyes with proliferative diabetic retinopathy (PDR) were similar to those of eyes with NPDR in the high-*P*-ratio group. **C, D, E**, Scatter plots of eyes with or without each 4-2-1 fundus finding. Hem = > 20 intraretinal hemorrhages in each of the 4 quadrants; VB in ≥ 2 quadrants; and intraretinal microvascular abnormalities in ≥ 1 quadrants. IRMA = intraretinal microvascular abnormalities; VB = venous beading.

$$\text{P ratio} = \frac{\text{The number of NPSs in APD(PDR) but not in APD(NPDR)}}{\text{The total number of NPSs}}$$

$$\text{N ratio} = \frac{\text{The number of NPSs in APD(NPDR) but not in APD(PDR)}}{\text{The total number of NPSs}}$$

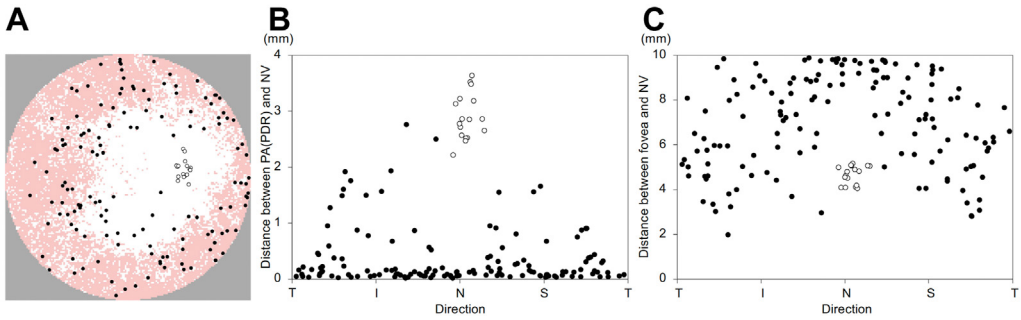

Figure 6. Association between retinal neovascularization (NVE) and areas with probabilistic differences (APD) between eyes with nonproliferative diabetic retinopathy (NPDR) and proliferative diabetic retinopathy (PDR) (APD[PDR]). **A**, The locations of APD(PDR) and neovascularization (NV) are shown. The nasal quadrant is shown on the right-hand side. **B**, The directions of NVs and their distances to the nearest square in the APD(PDR) are shown. Most NVEs are within or near the APD(PDR). **C**, The distances between the foveal center and NVs. The NVEs in the inferotemporal and superotemporal quadrants are nearest to the foveal center and those in the nasal quadrant are furthest. The white circle represents neovascularization of the disc. The black circle represents NVEs. I = inferior; N = nasal; S = superior; T = temporal.

underestimated or overestimated because of the evaluation of the NPSs. Fourth, the thresholds for the APD may have affected the calculations of the *P* ratios. Future multicenter studies should confirm the generalizability in the image acquisition, processing, and analytic methods.

In summary, we defined clinically significant NPA in DR on widefield OCTA images. Stochastic methods revealed the unique distribution of the APD(PDR) and concomitant NVEs, which may depend on the nonuniform vascular architecture.

Footnotes and Disclosures

Originally received: June 17, 2022.
Final revision: October 26, 2022.
Accepted: October 26, 2022.
Available online: November 2, 2022.Manuscript no. XOPS-D-22-00130R2.

Department of Ophthalmology and Visual Sciences, Kyoto University Graduate School of Medicine, Kyoto, Japan.

Disclosure(s):

All authors have completed and submitted the ICMJE disclosures form.

The author(s) have made the following disclosure(s):

Supported by a grant-in-aid for Scientific Research of the Japan Society for the Promotion of Science (grant no.: 20K09788). The funding organization had no role in the design or conduct of this research.

HUMAN SUBJECTS: Human subjects were included in this study. Kyoto University Graduate School and Faculty of Medicine Ethics Committee approved the study. All research adhered to the tenets of the Declaration of Helsinki. All participants provided informed consent.

No animal subjects were used in this study.

Author Contributions:

Conception and design: Kawai, Murakami

Analysis and interpretation: Kawai, Murakami, Mori, Tsujikawa

Data collection: Kawai, Murakami, Mori, Ishihara, Dodo, Terada, Nishikawa, Morino, Tsujikawa

Obtained funding: Murakami

Overall responsibility: Kawai, Murakami

Abbreviations and Acronyms:
APD = areas with probabilistic differences; **DR** = diabetic retinopathy; **FA** = fluorescein angiography; **IQR** = interquartile range; **IRMA** = intraretinal microvascular abnormality; **NPA** = nonperfusion area; **NPDR** = nonproliferative diabetic retinopathy; **NPS** = nonperfusion square; **NV** = neovascularization; **NVD** = neovascularization of the disc; **NVE** = retinal neovascularization; **OCTA** = OCT angiography; **PDR** = proliferative diabetic retinopathy; **PRP** = panretinal photocoagulation; **RPC** = radial peripapillary capillary; **VA** = visual acuity.

Keywords:
Diabetic retinopathy, Nonperfusion areas, Neovascularization, Semiautomatic quantification, Widefield OCT angiography.

Correspondence:
Tomoaki Murakami, MD, PhD, 54 Shougoin Kawahara-cho, Sakyo-ku, Kyoto 606-8507, Japan. E-mail: mutomo@kuhp.kyoto-u.ac.jp.

References

1. Yau JWY, Rogers SL, Kawasaki R, et al. Global prevalence and major risk factors of diabetic retinopathy. *Diabetes Care*. 2012;35:556–564.
2. Antonetti DA, Klein R, Gardner TW. Diabetic retinopathy. *N Engl J Med*. 2012;366:1227–1239.
3. Early Treatment Diabetic Retinopathy Study Research Group. Fluorescein angiographic risk factors for progression of diabetic retinopathy. ETDRS report number 13. *Ophthalmology*. 1991;98(suppl 5):834–840.
4. Morino K, Murakami T, Dodo Y, et al. Characteristics of diabetic capillary nonperfusion in macular and extramacular white spots on optical coherence tomography angiography. *Invest Ophthalmol Vis Sci*. 2019;60:1595–1603.

5. Kawai K, Uji A, Murakami T, et al. Image evaluation of artificial intelligence−supported optical coherence tomography angiography imaging using OCT-AI device in diabetic retinopathy. *Retina*. 2021;41:1730−1738.
6. Dodo Y, Murakami T, Suzuma K, et al. Diabetic neuroglial changes in the superficial and deep nonperfused areas on optical coherence tomography angiography. *Invest Ophthalmol Vis Sci*. 2017;58:5870−5879.
7. Cheung CMG, Fawzi A, Teo KY, et al. Diabetic macular ischaemia—a new therapeutic target? *Prog Retin Eye Res*. 2022;89:101033.
8. Early Treatment Diabetic Retinopathy Study Research Group. Classification of diabetic retinopathy from fluorescein angiograms. ETDRS report number 11. *Ophthalmology*. 1991;98: 807−822.
9. Jia Y, Tan O, Tokayer J, et al. Split-spectrum amplitude-decorrelation angiography with optical coherence tomography. *Opt Express*. 2012;20:4710−4725.
10. Spaide RF, Fujimoto JG, Waheed NK, et al. Optical coherence tomography angiography. *Prog Retin Eye Res*. 2018;64:1−55.
11. Couturier A, Rey PA, Erginay A, et al. Widefield OCT-angiography and fluorescein angiography assessments of nonperfusion in diabetic retinopathy and edema treated with anti-vascular endothelial growth factor. *Ophthalmology*. 2019;126:1685−1694.
12. Tan B, Chua J, Lin E, et al. Quantitative microvascular analysis with wide-field optical coherence tomography angiography in eyes with diabetic retinopathy. *JAMA Netw Open*. 2020;3:e1919469.
13. Wang FP, Saraf SS, Zhang Q, et al. Ultra-widefield protocol enhances automated classification of diabetic retinopathy severity with OCT angiography. *Ophthalmol Retina*. 2020;4: 415−424.
14. Wilkinson CP, Ferris FL, Klein RE, et al. Proposed international clinical diabetic retinopathy and diabetic macular edema disease severity scales. *Ophthalmology*. 2003;110:1677−1682.
15. Kadomoto S, Uji A, Muraoka Y, et al. Enhanced visualization of retinal microvasculature in optical coherence tomography angiography imaging via deep learning. *J Clin Med*. 2020;9: 1322.
16. Canny J. A computational approach to edge detection. *IEEE Trans Pattern Anal Mach Intell*. 1986;8:679−698.
17. Russell JF, Flynn HW, Sridhar J, et al. Distribution of diabetic neovascularization on ultra-widefield fluorescein angiography and on simulated widefield OCT angiography. *Am J Ophthalmol*. 2019;207:110−120.
18. Rabiolo A, Cicinelli MV, Corbelli E, et al. Correlation analysis between foveal avascular zone and peripheral ischemic index in diabetic retinopathy: a pilot study. *Ophthalmol Retina*. 2018;2:46−52.
19. Silva PS, dela Cruz AJ, Ledesma MG, et al. Diabetic retinopathy severity and peripheral lesions are associated with nonperfusion on ultrawide field angiography. *Ophthalmology*. 2015;122:2465−2472.
20. Jiang AC, Srivastava SK, Hu M, et al. Quantitative ultra-widefield angiographic features and associations with diabetic macular edema. *Ophthalmol Retina*. 2020;4:49−56.
21. Alibhai AY, de Pretto LR, Moult EM, et al. Quantification of retinal capillary nonperfusion in diabetics using wide-field optical coherence tomography angiography. *Retina*. 2020;40: 412−420.
22. Cardillo Piccolino F, Zingirian M, Mosci C. Classification of proliferative diabetic retinopathy. *Graefes Arch Clin Exp Ophthalmol*. 1987;225:245−250.
23. Henkind P. Radial peripapillary capillaries of the retina. I. Anatomy: human and comparative. *Br J Ophthalmol*. 1967;51: 115−123.
24. Uchitomi D, Murakami T, Dodo Y, et al. Disproportion of lamellar capillary non-perfusion in proliferative diabetic retinopathy on optical coherence tomography angiography. *Br J Ophthalmol*. 2020;104:857−862.
25. Balaratnasingam C, An D, Sakurada Y, et al. Comparisons between histology and optical coherence tomography angiography of the periarterial capillary-free zone. *Am J Ophthalmol*. 2018;189:55−64.
26. Yasukura S, Murakami T, Suzuma K, et al. Diabetic nonperfused areas in macular and extramacular regions on wide-field optical coherence tomography angiography. *Invest Ophthalmol Vis Sci*. 2018;59:5893−5903.
27. Petersen L, Bek T. The oxygen saturation in vascular abnormalities depends on the extent of arteriovenous shunting in diabetic retinopathy. *Invest Ophthalmol Vis Sci*. 2019;60: 3762−3767.
28. Fan W, Nittala MG, Velaga SB, et al. Distribution of nonperfusion and neovascularization on ultrawide-field fluorescein angiography in proliferative diabetic retinopathy (RECOVERY study): report 1. *Am J Ophthalmol*. 2019;206:154−160.
29. Wenner Y, Wismann S, Preising MN, et al. Normative values of peripheral retinal thickness measured with Spectralis OCT in healthy young adults. *Graefes Arch Clin Exp Ophthalmol*. 2014;252:1195−1205.
30. Fukushima Y, Okada M, Kataoka H, et al. Sema3E-PlexinD1 signaling selectively suppresses disoriented angiogenesis in ischemic retinopathy in mice. *J Clin Invest*. 2011;121: 1974−1985.
31. Okabe K, Kobayashi S, Yamada T, et al. Neurons limit angiogenesis by titrating VEGF in retina. *Cell*. 2014;159: 584−596.
32. Russell JF, Al-Khersan H, Shi Y, et al. Retinal nonperfusion in proliferative diabetic retinopathy before and after panretinal photocoagulation assessed by widefield OCT angiography. *Am J Ophthalmol*. 2020;213:177−185.
33. Stefánsson E, Hatchell DL, Fisher BL, et al. Panretinal photocoagulation and retinal oxygenation in normal and diabetic cats. *Am J Ophthalmol*. 1986;101:657−664.
34. Aiello LP, Avery RL, Arrigg PG, et al. Vascular endothelial growth factor in ocular fluid of patients with diabetic retinopathy and other retinal disorders. *N Engl J Med*. 1994;331: 1480−1487.
35. Mendrinos E, Mangioris G, Papadopoulou DN, et al. Retinal vessel analyzer measurements of the effect of panretinal photocoagulation on the retinal arteriolar diameter in diabetic retinopathy. *Retina*. 2010;30:555−561.
36. Bennett AG, Rudnicka AR, Edgar DF. Improvements on Littmann's method of determining the size of retinal features by fundus photography. *Graefes Arch Clin Exp Ophthalmol*. 1994;232:361−367.
37. Sampson DM, Gong P, An D, et al. Axial length variation impacts on superficial retinal vessel density and foveal avascular zone area measurements using optical coherence tomography angiography. *Invest Ophthalmol Vis Sci*. 2017;58: 3065−3072.